PROCEEDINGS OF SCIENCE

A new Recoil Proton Telescope with CMOS-pixels for fast neutron metrology

Daniel Husson*, **Stephane Higueret, The Duc Lê, Mathieu Trocmé**
daniel.husson@ires.in2p3.fr
Institut Pluridisciplinaire Hubert Curien / UMR 7178, 23 rue du loess, 67037 Strasbourg (F)

Amokrane Allaoua, Lena Lebreton
Laboratory for Neutron Metrology and Dosimetry, IRSN, 13115 St Paul lez Durance (F)

A new type of telescope for fast neutrons is under development. The device comprises thin CMOS pixel sensors for accurate tracking of recoil protons, followed by a thick Si(Li) diode to measure their energy. The CMOS Recoil Proton Telescope (CMOS-RPT) is to be installed at the AMANDE facility in Cadarache, an accelerator-driven source of mono-energetic neutrons, in the range 2 keV - 20 MeV.

After general physics of H(n,p) elastic diffusion, we present the advantages to be expected from pixel technology. The technical choices for the telescope are discussed in parallel with Monte Carlo simulation studies, and special attention is given to the critical issue of multiple scattering of non relativistic protons. The very first experimental results obtained with the EUDET telescope in three mono-energetic lines at AMANDE are presented.

17th International Workshop on Vertex detectors
July 28 - 1 August 2008
Uto Island, Sweden

*Speaker.

PoS(VERTEX 2008)033

Contents

1. Introduction

Neutron physics covers a wide range of fundamental and applied subjects, from stellar models to material studies with cold neutrons or spallation sources for nuclear waste management, and a strong demand emerges for well calibrated neutron sources. The LMDN Laboratory in Cadarache (Laboratoire de Métrologie et Dosimétrie des Neutrons) has recently commissioned the AMANDE facility [1], an accelerator-driven source of monoenergetic neutrons in a wide energy range (2 keV-20 MeV). A neutron spectrometer of metrological quality was needed, and the IPHC in Strasbourg

(Institut Pluridisciplinaire Hubert Curien) proposed, for the highest energy region of this facility [7 – 20 MeV], a new technology based on CMOS pixels.

One of the key features of this approach is the recent possibility of thinning CMOS sensors down to 50 μm, opening the way to micrometer-precise tracking of low energy recoil protons with a moderate effect of Coulomb scattering. We target therefore an unprecedented combination of high efficiency and energy resolution.

2. Physics of elastic neutron scattering

Detection of recoil nuclei from elastic scattering is widely used, since the diffusion cross section is of $\sigma_{(n,p)} \simeq 20\ bn$ at 100 keV (and still 1 bn at 10 MeV). This quite high cross section leads to sizeable conversion probabilities in hydrogen-rich converters, typically $10^{-3}\ proton/neutron$ for a 1-mm thick foil of $n_H = 10^{22}\ cm^{-3}$ hydrogen atoms content.

2.1 The angle-energy relation

At MeV energies, the elastic scattering of neutrons by nuclei of mass A is isotropic in the center-of-mass (CM) of the (n,A) system. Simple kinematics shows that the recoil nucleus is scattered at the angle θ_A with the energy:

$$E_A(\theta_A) = [4A/(1+A)^2] \cdot E_n \cdot cos^2(\theta_A) \tag{2.1}$$

High energy transfers with low mass isotopes is the working principle of light moderators in nuclear plants. If the recoil nucleus is a proton (A=1), the energy transfer to the recoil is maximal:

$$E_p(\theta_p) = E_n \cdot cos^2(\theta_p) \tag{2.2}$$

In a standard telescope experiment, one measures charged particle tracks therefore the recoil angle θ_p. With our device (see below) the proton energy E_p is also measured, and this combination allows to calculate the initial neutron energy E_n.

2.2 Angular distributions

Isotropy means a uniform distribution of $cos(\theta_n)$ in the center-of-mass of the (n,p) system. For scattering of a particle of mass m on a mass M, the classical formula from CM to the laboratory (LAB) is: $tan(\theta^{LAB}) = sin(\theta^{CM})/[m/M + cos(\theta^{CM})]$. In our case, it reduces to a simple relation between the proton angles: $\theta^{LAB} = \theta^{CM}/2$. As a consequence, the random variable which is uniformly distributed is the squared cosine $cos^2(\theta_p)$ in LAB, therefore a uniform distribution of the proton energy.

2.3 The European benchmark

A reference place in Europe for neutron metrology is the PTB laboratory [2] in Braunschweig (Germany), which uses a gas proportional chamber to track the protons generated in a plastic foil. The gas cell selects only the recoil protons at very small angles ("zero degree cell") and a diode measures the remaining proton energy.

The MCNPX code [3] is a standard package for neutrons, and our group already used it for CMOS response to alpha particles [4]. For MeV neutrons, we have simulated the complete distribution of recoil proton angles (**Fig. 1**), including, for protons emitted at large angles, the probability of being stopped inside the converter. Obviously, a zero-degree detector rejects most of the recoils, with a resulting efficiency of only 10^{-5} p/n at PTB [2].

In the CMOS-RPT project, we aim at increasing the detection solid angle, in order to enhance the efficiency significantly.

3. Advances with pixel technology

3.1 Efficiency: the DOSIPIX-N results

Our group has already successfully detected recoil protons with a CMOS pixel sensor [5], with the project of designing a compact electronic dosimeter called the DOSIPIX-N. This measurement has been performed with a calibrated AmBe source [8]. An efficiency of $\varepsilon = 1.5 \cdot 10^{-3}$ has been reached, close to the theoretical maximum. We could reach this high efficiency by detecting the almost complete distribution of the recoil protons ($\Delta\Omega/2\pi \simeq 95\%$), as the converter foil was in contact with the sensor. As neither angle nor energy measurement were made, it was not possible to remove properly the inelastic contributions, thus a somewhat overestimated efficiency.

3.2 Gamma background

In addition to high efficiency to MeV protons, another important aspect of CMOS sensors is their limited thickness (some tens of microns), making them highly transparent to gamma photons [5]. The gamma background is a major concern for all neutron sources, with for instance 0.57 γ for each neutron in a standard AmBe source [6]. Discrimination between gamma photons and neutrons is uneasy, but thin and light detectors like CMOS sensors are naturally transparent to such photons because of their long interaction length: typical photons of an AmBe source ($E_\gamma = 4,483\ MeV$) cross the 15 μm epitaxial silicon with a cm-long interaction length ($L \simeq 10\ cm$). Combining the 0.57 ratio to this low interaction probability, the expected detection ratio photon/neutron is of less than 0.06, and detailed simulations with the MCNPX code confirm this estimation.

Moreover, secondary electrons from MeV photons are relativistic: the charge released by fast electrons is a factor of 100 below the charge released by recoil protons in the EPI layer, and the two charge distributions are clearly distinguished [7]. This nice feature makes CMOS devices very competitive for neutron metrology, compared to thick detectors [5].

3.3 Theoretical tracking precision

We can differentiate the angle-energy relation (Eq.2.2) to obtain the RMS error on the reconstructed energy. As the two measurements are independant, one gets:

$$\sigma_{E_n}/E_n = [(\sigma_{E_p}/E_p)^2 + 4 \cdot tan^2(\theta) \cdot \sigma_\theta^2]^{1/2} \tag{3.1}$$

Since the proton energy is measured in Si(Li) diodes with a 0.1 % precision, the error on neutron energy will be dominated by the second term, and the relative error reduces to:

$$\sigma_{E_n}/E_n \simeq 2 \cdot tan(\theta) \cdot \sigma_\theta \tag{3.2}$$

It has to be noticed that the relative error on the energy depends on the absolute error on the angle, and this stresses the advantage of tracking the protons at the micron level. Pixels of pitch p with digital readout lead to $\sigma_x = p/\sqrt{12}$, but a much better precision can be obtained using the analog information (e.g. center-of-gravity algorithm [9]). This project could benefit from pixel detectors kindly provided by the STAR collaboration. With $p = 30\ \mu m$ pixels, the digital precision is $\sigma_x = 8.66\ \mu m$, and in CMOS pixels arranged in consecutive planes distant of $d = 1\ cm$, the absolute error on measured angles would be as small as $\sigma_\theta \leq 9 \cdot 10^{-4}$.

The $tan(\theta)$ term in Eq.3.2 is making in favour of small angles, at the expense of conversion efficency. An acceptance angle of 45^o corresponding to $\Delta\Omega/2\pi \simeq 30\%$ would be a reasonable trade off, leading to an unprecedented precision on neutron energy (neglecting multiple scattering).

4. Limitating effects

4.1 Coulomb scattering

Unfortunately, this theoretical precision is strongly affected by Coulomb diffusion. As MeV protons are far from being at the minimum of ionisation, they undergo important multiple scattering. Following the Highland model [10], the RMS deviation angle increases like the inverse of the particle momentum. After crossing a material layer of thickness x and radiation length X_0, this angle is given by:

$$\sigma_\theta = 20\ MeV/c/(p \cdot \beta) \cdot (x/X_0)^{(1/2)} \cdot [1 + (1/9) log_{10}(x/X_0)] \tag{4.1}$$

A 20 MeV proton has a velocity of $\beta = 0.203$ (Lorentz factor). With a sensor thickness $x = 50\ \mu$m or $x/X_0 = 5.34 \cdot 10^{-4}$, the scattering angle predicted by Highland is 7.7 mrad after crossing a single plane (8.5 mrad including the SiO_2 layer). After three consecutive silicon planes, this model predicts a cumulated scattering effect of less than 15 mrad (at normal incidence). This estimation is in agreement with simulations performed with the MCNPX Monte-Carlo code (**Fig. 2**).

As expected, the final precison is significantly lowered by Coulomb scattering. Nevertheless, a 3-planes system made of thin silicon sensors can reach the energy precision required for metrology: Targeting a 40^o to 45^o acceptance angle to optimize the efficiency, the CMOS-RPT should be able to reconstruct the neutron energy at 5%.

Multiple scattering of MeV protons is the dominant contribution to the worsening of the resolution: for an inter-sensor distance of $d = 1\ cm$, the projected lateral deviation from one sensor to the next is 85 μm (one standard deviation at 20 MeV). Clearly, there will be no net gain in having a very fine pixel granularity.

4.2 Inelastic events

We have to take care of several inelastic reaction channels, mostly (n,p) or (n,α) on all the present nuclei, ^{28}Si and ^{16}O (sensors plus oxyde layers), ^{14}N from air and ^{12}C (polyethylene converter and PCB cards). All these channels have their threshold energy between 1 and 8 MeV.

Each one has a cross-section well below the elastic channel, but the total inelastic cross section reaches the elastic $H(n,p)$ above 10 MeV (**Fig. 3**). Backscattering from the thick diode is also to be considered.

In fact, most of these parasitic signals can be removed, for instance α particles are easely stopped by thin layers of materials, and none of them is able to cross the entire telescope. The request of crossing all the sensor planes is a stringent constraint, and only fast protons generated before the first epitaxial layer can perfectly simulate true elastic events. This "complete-track request" eliminates for instance the numerous events generated in the PCB cards, as well as secondaries generated in next-to-first planes. For parasitic events coming from the air layer in front of the converter, a shielding-up of the polyethylene foil is foreseen.

A second strategy to remove these unwanted events is to set a cut on the energy measured by the diode. This method seems very efficient against backscattering, as can be seen in simulations (**Fig. 4**). Two programmable energy thresholds (low and high) will be used for the Si(Li) diode.

The combination of these three methods (complete track, shielding and diode threshold) should remove most of these events.

5. Experimental results with the EUDET telescope

In order to check the most critical issues of the project (track reconstruction, multiple scattering, inelastic events), a preliminary experiment has been performed with an existing device.

5.1 EUDET configuration

The EUDET telescope is a modular beam-test device for detector developments in particle physics [11]. The configuration we used was a subset of the complete telescope, including only four planes of sensors. The MIMOSA-18 chips, of 10 μm pitch, have been thinned down to about 60 ± 5 μm. Each sensor has a sensitive area of 5.1×5.1 mm^2. Our spacing between sensors was d_{12}=3 mm, d_{23}=15 mm and d_{34} =3 mm, thus a maximal track angle of 13.4^o. The 100 μm polyethylene converter foil was glued in front of the first plane, at less than 2 mm distance.

This geometry (23×5.1) offered an acceptance of $\Delta\Omega/2\pi \simeq 0.7\%$.

5.2 AMANDE runs

This EUDET configuration was tested in AMANDE in april 2008. No diode was used and the telescope was runned without any trigger signal. The EUDET system was set at about 75 cm of the tritium-rich target that generates neutrons through the (d,n) inelastic reaction. The AMANDE facility allows to change the target-to-detector angle with respect to the accelerator axis, hence to modify the neutron energy without changing the machine settings. In our 5-days experiment, we tested three energies, namely 14.8 MeV, then 19 MeV and a couple of hours at 5 MeV. Neutron fluences depend sharply on machine parameters, and in these experiments, the delivered fluences were between 400 and 8000 $n \cdot cm^{-2} \cdot s^{-1}$.

5.3 Main results

The EUDET telescope is designed for charged beams, and the DAQ system has a sizable (and variable) dead time in the non-triggered mode. This prevented any precise study of efficiency, but

the maximal typical detection rate was 1.6 proton/s, compatible with an estimated efficiency of some 0.1×10^{-3}.

a) Acceptance: The time coincidences between different CMOS planes have been checked in the following progression, $(P1+P2)$, $(P1+P2+P3)$ and $(P1+P2+P3+P4)$. For a track emerging in the center of the converter, we can define the relative solid angles viewed by each plane: setting $\Omega_1 = 100\%$ for events crossing $(P1)$, the geometry gives $\Omega_2 = 28.1\%$, $\Omega_3 = 2.06\%$ and $\Omega_4 = 1.56\%$. This has to be compared to the measured coincidences.

- at E_n=14.8 MeV, the relative fraction of coincidences was of 21.97% in $(P1+P2)$, 2.95% in $(P1+P2+P3)$ and 0.84% in all four sensors. This excellent agreement proves that all tracks emerge really from the polyethylene converter, with negligible secondary events.

- at E_n=19 MeV on the contrary, we observe the fraction of coincidences decreasing very slowly (in the same order, 100, 93, 75 and 66 %). This indicates a strong generation of inelastic events inside the *Si* sensors themselves, and a careful analysis is needed here.

- at E_n=5 MeV, the inelastic events disappear completely, but very few of these slow protons cross all four planes and we lack statistics, as only 15 events were recorded. Nevertheless, the sucessful detection of recoils at 5 MeV makes us confident that a two-planes geometry with higher acceptance can be useful even at these energies.

b) Tracking:

A nice track recorded in the four planes with little scattering is depicted in **Fig. 5**. The error bars are calculated as follows: plane $(P1)$ has only the intrinsic pixel error $\sigma_x = \sigma_y \simeq 3\ \mu m$. This precision is already higher than needed, and we didn't use the analog information of the MIMOSA 18. There is also a scattering effect inside the converter, however small enough as the radiation length of $(CH_2)_n$ is $X_0 = 46\ cm$. For all sensors, this first error is added in quadrature with the scattering angle from the Highland formula. This cumulative procedure is useful for a chi-square search of the good tracks. After this selection process, the true uncertainity on the reconstructed angle is taken from $(P1)$ and $(P2)$ alone.

Preliminary results of this analysis are summarized in **Fig. 6**. We define a deflection angle $\Delta\theta$ measured in $(P3)$ relative to the first segment $(P1,P2)$, and a new one in $(P4)$ in the same way. The scattering angle is calculated separately from X and Y coordinates, as the two projections must behave like independent random variables. Despite low statistics at 14.8 MeV, the first plot shows the absence of correlation between $\Delta\theta_X$ and $\Delta\theta_Y$. The mean value centered on zero is a good check of the alignment of the EUDET telescope. The reconstructed deflection angle distribution shows non-gaussian tails, a well known effect corresponding to "plural scattering" [13]. The final plot is the fully three-dimensional scattering angle. The mean value includes the large tail, but even the peak value is a bit higher than expected. Several corrections have to be included into the analysis (true thickness of sensors and oxyde, energy losses, complete clustering, sensor z-positions, etc.)

6. The CMOS-RPT prototype

6.1 Sensors

We chose to design this prototype with available sensors as spares of the STAR collaboration [12]): with a pitch of 30 μm and an active area of 2 $\times$ 1 cm^2, the total of 640×320 pixels are

readout with two independant channels. The CMOS-RPT will be made of three tracking planes, each of some 10^5 *pixels*, and a thick diode.

The MIMOSTAR3L chips have a 20 μm thick epitaxial layer and are designed in the AMS-0.35-OPTO-2006 technology. Initially 300 μm thick, they have been thinned down to 50 μm and mounted on specially designed PCB support-cards (**Fig. 7**), with a void below each sensor.

6.2 Global acceptance

We pushed the mechanical design of the supporting PCBs to a very close spacing of 0.6 cm between sensors, and the entrance window of the Si(Li) diode is at 1 mm of the last CMOS plane: this geometry leads to a high acceptance solid angle of $\Delta\Omega/2\pi = 6.7\%$. A track at maximal angle will be seen at 35.5^o, and for these recoil protons $E_p/E_n = 0.66$.

6.3 Diode

The Si(Li) diode is 3 *mm* thick in order to stop 20 MeV protons. Its active area is of 2 cm^2 to match the pixel sensors. The full polarisation bias is 450 V. Its response time has been shaped to 1 μs to maximize rejection of pile-ups due to parasitic hits, as neutrons will interact everywhere inside the telescope, mostly in the diode itself.

6.4 Mechanics and digital board

The mechanical structure supporting the three vertical sensors+PCBs and the diode PCB (**Fig. 7**) is the data processing digital board. To process the high-throughput parallel data delivered by the three sensors, we designed a special architecture to buffer the input signal with a high-density (131K) 36-bit FIFO. In this first prototype, only one channel per sensor will be used, therefore a single memory. A fast reading is necessary to remove the fake coincidences generated by inelastic events, especially inside the thick diode: as can be seen on **Fig. 3**, the inelastic cross section in silicon is only 1/3 of the elastic channel, and the total silicon thickness will be 3.15 *mm*. With 102400 pixels per sensor, a 12 bits resolution and a clock frequency of 40 MHz, the readout cycle of one sensor is of 40 *ms*. This will be fast enough to remove all pile-ups: taking a diode efficiency to neutrons of 10^{-2}, we expect up to 80 fake hits per second at maximal fluence of 8000 $n \cdot cm^{-2} \cdot s^{-1}$ (at 75 cm of the target).

The system is designed for zero dead time. Data sparsification will be done inside a FPGA with the help of the FIFO memory to reduce the data rate. The supporting board is set to send the parallel data to an acquisition board inside a PC (a future upgrade will interface the system by TCP/IP).

7. Conclusion and acknowledgments

Both simulation studies and preliminary experimental results point to the feasibility of our concept of CMOS-RPT for fast neutrons. The project could be managed at reasonable cost as existing sensors were available. The technical choices are optimized for the AMANDE facility at Cadarache, but in case of good performance in energy resolution, we will test its spectrometric capabilities in other sources. The prototype is currently being assembled, and is to be tested with neutrons in spring of 2009. The results will be presented elsewhere.

We warmly acknowledge the EUDET team: W.Dulinski, D.Haas and E.Corrin for fast and professional commissioning of the telescope. It is a pleasure to thank people in Cadarache involved in the AMANDE machine: V.Gressier, A.Martin and M.Pepino, as well as C.Monnin-Parietti for her early support in the project. In Strasbourg, we are greatly indebted to several people of the micro-electronics group, especially Ch.Hu for kindly providing detectors, and also to our student M.Taverne for his enthusiastic contribution.

References

[1] V.Gressier, L.Lebreton et al.,*AMANDE, a new facility for mono-energetic neutron fields production between 2 keV and 20 MeV*; Rad.Prot.Dosim.,Vol.110,n^o1-4(2004)49

[2] H.J.Brede et al.,*The Braunschweig accelerator facility for fast neutron research*; Nucl.Instr.Meth.193, Vol.3(1982)635

[3] http://mcnpx.lanl.gov

[4] A.Nachab, D.Husson et al.,*MCNPX simùlations for alpha particle detection by CMOS active pixels*; Nucl.Instr.Meth. B225(2004)418

[5] M.Trocmé, D.Husson et al.,*A new compact device for efficient neutron counting using a CMOS active pixel sensor*; Rad.Meas.Vol43,2-6(2008)1100

[6] Z.Liu et al.,*The 4.438 MeV gamma to neutron ratio for the Am-Be neutron source*; Appl.Rad.and Isotopes 65 (2007)1318.

[7] M.Vanstalle, private communication and Proc.11th,NEUDOS Conference (Oct.2009).

[8] H.Kluge and K.Weise,*The neutron energy spectrum of an AmBe (α,n) source*; Rad.Prot.Dosim.,Vol.2,2(1982)85.

[9] J.Straver, R.Turchetta et al.,*One micron spatial resolution with silicon strip detectors*; Nucl.Instr.Meth. A348,(1994)485

[10] G.R.Lynch and O.I.Dahl,*Approximations to multiple Coulomb scattering*; Nucl.Instr.Meth. B58(1991)6

[11] A.Bulgheroni, *First test beam results for the EUDET pixel telescope*; NSS Conf.Record 2007, pp1878-1884, Oct.2007.

[12] B.I.Abelev et al.,*STAR collaboration*; Nucl.Phys.A,Vol.774,7(2006)956

[13] William T.Scott, *Theory of small angle multiple scattering of fast charged particles*; Rev.Mod.Physics 35,2(1963)231

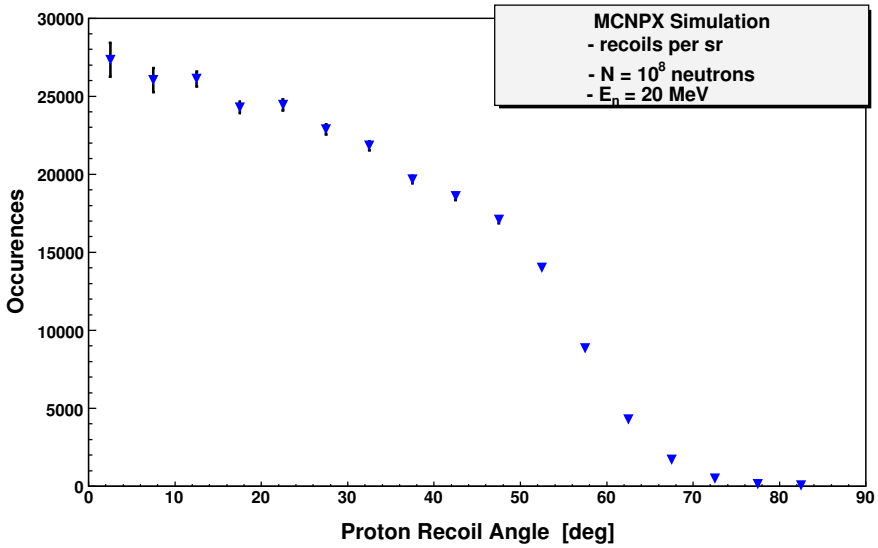

Figure 1: Angular distribution (per steradian) of the detected protons after a 100 μm thick polyethylene converter (MCNPX simulation).

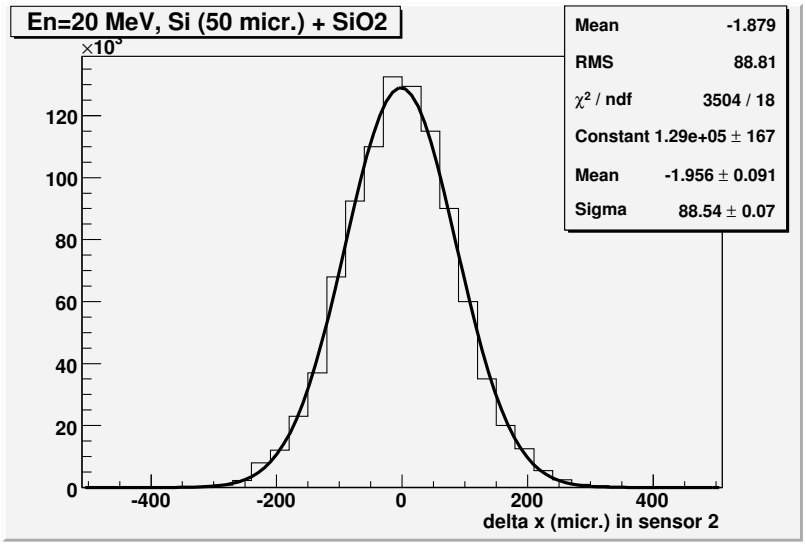

Figure 2: Simulation of the Coulomb scattering from one sensor plane to the next (at 1 cm distance). MCNPX uses a nearly gaussian model (fit superposed).

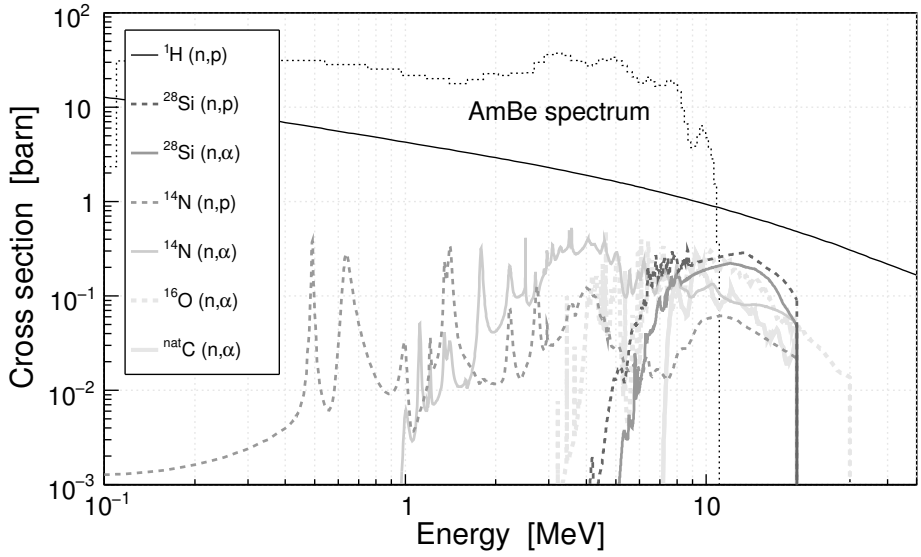

Figure 3: Inelastic channels compared to the dominant H(n,p) reaction.

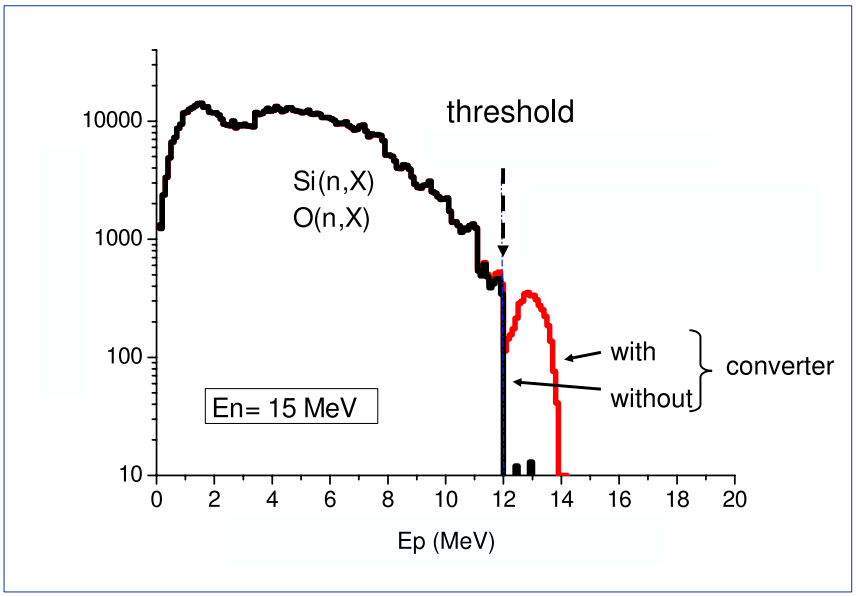

Figure 4: MCNPX simulation of diode signal with and without polyethylene. A suitable threshold on the diode removes most of the inelastic signals.

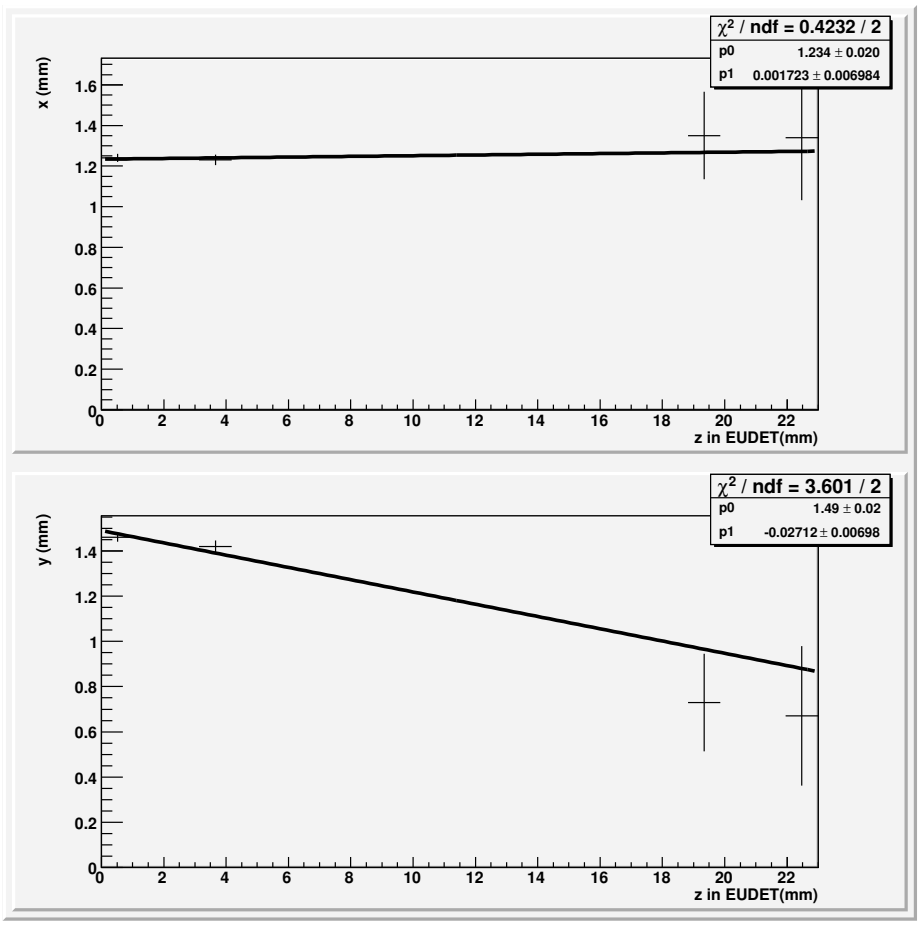

Figure 5: A 14 MeV proton track reconstructed in EUDET, projected on X (above) and Y (below).

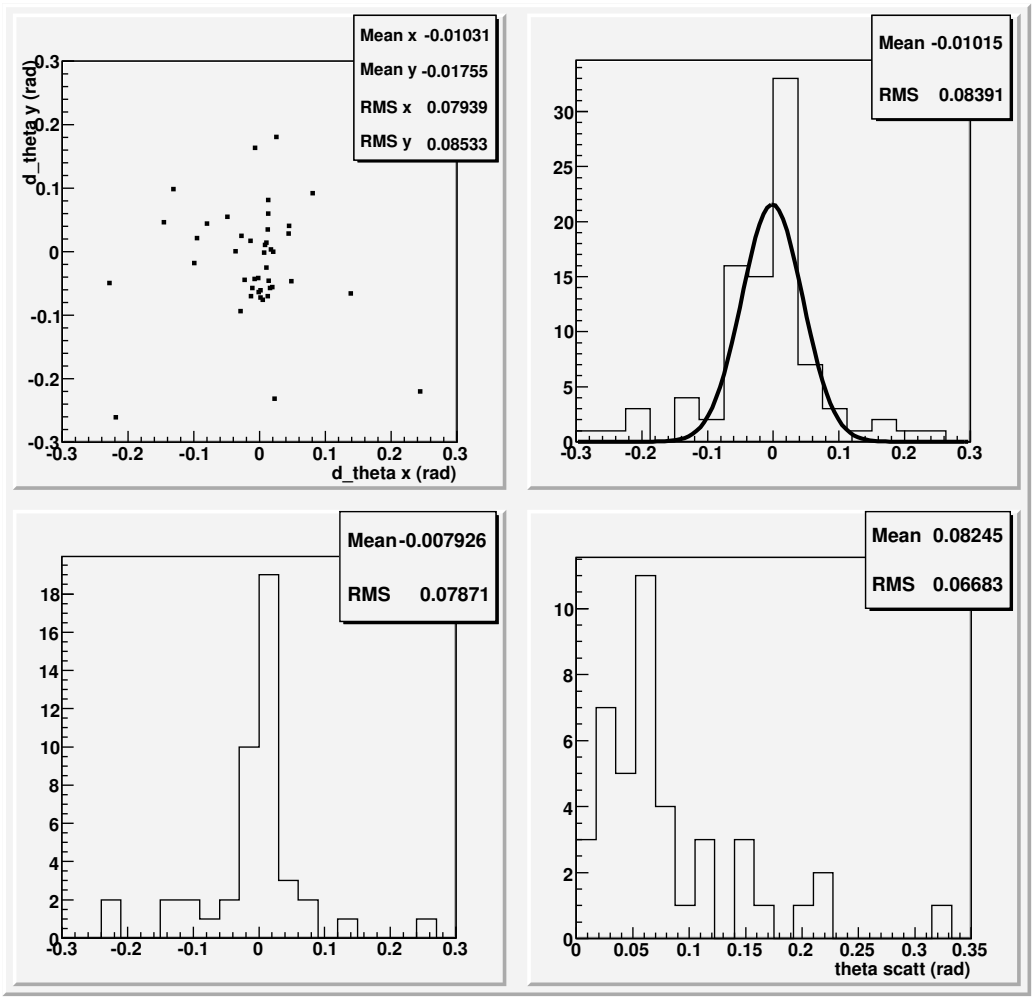

Figure 6: Angular deviations $\Delta\theta$ between consecutive planes. Top left: X versus Y projections (absence of correlation); Bottom left: X-projection (EUDET is well centered); Top right: fit of cumulated X and Y projections, showing non-gaussian tails; Bottom right: 3D deviation angles (in spherical coordinates).

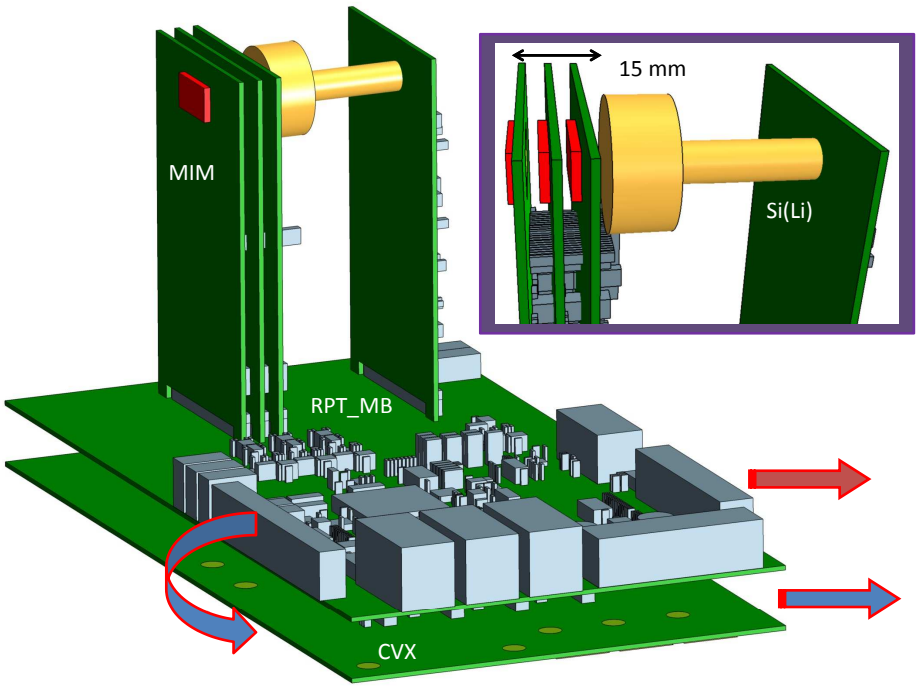

Figure 7: Geometry of the CMOS-RPT: three CMOS planes with 6 mm spacing and the thick Si(Li) diode (yellow). MB stands for motherboard, MIM for MIMOSTAR board.